

Evaluation of pressure distribution around the High-pressure gates using ANFIS

Hamidreza Sajadi*¹
Mohammadreza Kavianpour¹
Sepide Mostafavi¹

Abstract

The bottom outlet is essential for dams, controlling reservoir water volume, managing downstream flow, and discharging sediment. Understanding pressure distribution around the high-pressure gate is crucial for assessing risks like cavitation, vibrations, and down-pull forces. This paper presents a model for estimating pressure distribution around the Downpull Force of dams using an Adaptive Neuro-Fuzzy Inference System (ANFIS). The model was trained with laboratory data from physical models of the Ghezhgaleh Si, Alborz, Gotvand, Namroud, and Seymareh dams. Analysis revealed that pressure distribution around the bottom lip face of the gates varies from the vertical face and in the vertical direction for 80% and 90% of openings differ from other openings. Results demonstrate a significant reduction in the mean relative error of estimated vertical forces on the gates from 61.2% (using the Naudascher ratio) to 10.1%. Notably, this research uniquely estimates horizontal force levels with an average acceptable error of 5.3%, minimizing the need for costly laboratory modeling. This model's key advantage is its ability to estimate horizontal forces that typically require laboratory testing. Its high accuracy makes it preferable for designing high-pressure gate elevator jacks over standard methods and prior laboratory or numerical studies.

Keywords: High-pressure gate, Pressure distribution, down-pull force, ANFIS

Received: 15 December 2024; Accepted: 20 January 2025

1. Introduction

Invaluable structures like dams, ensuring the proper operation of hydraulic systems under various conditions is crucial. It's essential to maintain the functionality of the dam's hydraulic equipment and prevent damage, particularly to the bottom outlet and its gates, which are not easily repairable. Bottom outlets regulate water transfer from the dam to the downstream discharge point. Studying the high-pressure gate in dams is vital for safe downstream discharges and for emptying sediment from behind the reservoir. [1,2,3].

*Email: sajadi.hamidreza@gmail.com (Corresponding author)

¹ Faculty of Civil Engineering, K.N.Toosi University of Technology, Tehran, Iran.



The objectives of bottom outlet construction can be summarized as facilitating reservoir discharge, meeting downstream requirements, adjusting reservoir levels, enabling reservoir scouring, and assisting flood discharge systems. The critical role of the bottom outlet in the operation of large dams necessitates meticulous calculations of forces on the gates and hydraulic flow, along with the significant costs associated with construction, repair, and reconstruction. Performance analysis of outlet components, including channels, gates, and both inlet and outlet areas, is particularly crucial. In these dischargers, the upstream flow is under pressure while the downstream flow is at a free surface. Researchers have emphasized the free surface area due to the mixing of water and air, the design of air-feeding systems, and the risks of cavitation and shear stress caused by sedimentary flow over the duct wall [4]. Vertical sliding gates serve as high-pressure discharge control or emergency shutdown mechanisms for bottom outlet cross-sections [5]. Flow control gates at the bottom outlets of dams often face incompatible and hazardous dynamic conditions. Key contributors to bottom outlet failure include cavitation, duct damage, gate vibration, and the forces acting on them. Parameters like discharge, flow rate, hydrodynamic pressure, air concentration, and flow geometry can be crucial in assessing and preventing duct failure.

One of the discussed issues in pressurized ducts is the force acting on the gate. When fluid flows under the gate, a hydrostatic pressure is applied to the bottom edge, resulting from the pressure difference between the upper and lower gates. This creates either a downward or upward force on the gate. This resultant force, known as the Down-pull Force along with gate weight and friction force, determines the capacity of the hydraulic jack to raising and lowering the gate. Therefore, the estimation of hydrodynamic forces is one of the important issues in designing a High-pressure gate for high dams [6]. Since the forces acting on the gates are influenced by the pressure distribution on the gates, understanding the factors affecting the pressure distribution around the gates is an important and effective step in estimating the hydrodynamic force applied to them. Hydrodynamic forces are affected by various hydraulic and geometric parameters, which have been extensively researched through mathematical and experimental methods.

The results of the flow-through analysis under a gate and the Down-pull Force applied to the same gate have been presented by Nadascher et al. [7]. These results showed that apart from the bottom edge geometry of the gate, the flow rate through the gate also had a significant effect on the Down-pull Force.

Sagar stated that the geometrical properties of the gate including functional head, gate opening and gate edge geometry, boundary layer properties, and turbulence, influence the Down-pull Force applied to the High-pressure gate [8]. He and Tullis also examined the different forces applied to the gates when opening and closing them [9].

The hydrodynamic forces acting on the hydraulic gates were investigated by Nadascher using physical models. Parameters measured after reading were converted to dimensionless parameters using dimensional analysis and these parameters were displayed in different graphs. These diagrams are used to predict the forces acting on the gates. An empirical relation based on experiments has been proposed to estimate this force. Based on this empirical relationship, the Down-pull Force is calculated from the difference in pressure force applied to the upper and lower levels of the gate [10]:

$$F_1 = (\bar{\kappa}_t - \bar{\kappa}_b) B d \rho \frac{V_j^2}{2} \quad (1)$$

Where the F_1 down-pull force (or up-pull), $\bar{\kappa}_t$ The force factor on the upper edge of the gate, $\bar{\kappa}_b$ The force factor on the bottom edge of the gate, B Width of the valve, d thickness of the

valve, ρ Water density, V_j The compact jet velocity of flows under the gate.

The coefficients of force applied to the upper and lower surfaces of the gate ($\bar{\kappa}_b$ and $\bar{\kappa}_t$) are also defined as follows:

$$\bar{\kappa}_t = \frac{1}{Bd} \int_0^d \int_0^B \frac{h_t - h}{\frac{V_j^2}{2g}} dBdx = \frac{h_t - h}{\frac{V_j^2}{2g}} \quad (2)$$

$$\bar{\kappa}_b = \frac{1}{Bd} \int_0^d \int_0^B \frac{h_i - h}{\frac{V_j^2}{2g}} dBdx \quad (3)$$

Where h_t is the pressure head at the top surface of the gate and h_i is the pressure head is at the bottom surface of the gate. Coefficients $\bar{\kappa}_t$ and $\bar{\kappa}_b$ are presented in experimental diagrams by Nadauscher, based on channel and gate geometry, percentage of openings, and gate sealing.

Amorim and Andrade developed the use of a numerical model of incompressible viscous fluid flow controlled by a gate and also investigated the down-pull force applied to the gates [11]. Their numerical solution was based on the solution of Navier-Stokes equations and in order to consider the effects of turbulence, they used the k- ϵ model and finally compared the numerical modeling results with the experimental results. Sagar investigated the effect of gate edge geometry on cavitation, vibration, and down-pull force. His studies showed that the correct choice of angle of the gate edge has an important role in minimizing the occurrence of cavitation and the negative effects of vibration and also reducing the hydrodynamic force applied to the gate [12].

Alhashimi et al. presented a two-dimensional numerical model for estimating the down-pull force coefficient. The results showed that the lowest positive value of the down-pull force occurs in the gate position with the lower edge angle ($\theta = 35^\circ$) [13].

Up-to-date research in many laboratories and scientific centers around the world has investigated the influence of various parameters including flow rates, geometrical parameters, gate edge shape, and bottom edge direction by physical and numerical models [14,15,16,17].

Since the hydrodynamic pressure around the High-pressure gate is subject to hydraulic and geometrical parameters such as tunnel geometry, gate geometry, gate sealing, water head, and different gate openings, the hydrodynamic pressure estimation is based on numerical modeling method. The actual conditions of the upstream flow are very complex. Investigation of the studies on the distribution of pressure around the High-pressure gate and determining the forces applied to them indicate that further research is needed. However, laboratory models to determine the forces acting on gates and their hydraulic design are still the basis of many studies [19]. The use of artificial intelligence methods in the Adaptive neuro-fuzzy inference system (ANFIS) is another approach that has been considered in addition to numerical and laboratory studies in recent decades. These models provide a good response in simulating various processes such as hydrology and hydrogeology, reservoir management, and suspended sediment load estimation.

Since most studies on pressure distribution around High-pressure gates have focused on experimental and numerical modeling, it is necessary to investigate the effectiveness of conceptual methods such as the Adaptive neuro-fuzzy inference system for predicting pressure distribution around High-pressure gates. For this purpose, data from service and emergency

gates of physical models of Ghezghaleh Si, Alborz, Gotvand, Namroud and Emergency gates of physical models of Seymareh Dam, all made and tested by the Iranian Water Research Institute, were Used.

2. Laboratory data

This study utilized data from scaled physical models of Bottom outlets, with a scale of 1:10 to 1:15, created by the Iranian Water Research Institute (WRI). The models represent the Bottom outlets of the Ghezghaleh Si, Alborz, Gotvand, Namroud, and Seymareh dams. The Seymareh Dam features a rectangular service gate and an emergency gate, with the latter being the focus of this research. For the other dams, pressure distribution results for both service and emergency gates, all rectangular, were analyzed. Various piezometers were employed to measure mean pressure values, installed at different locations within the duct, including the inlet, gate body, grooves, walls, and floor. These piezometers connect to vertical manometers via hoses, allowing pressure values to be derived from the water column height. Adjustments are made for piezometer position effects and scale effects to obtain corresponding real-scale pressure values. A total of 648 data series were collected from nine models. Measurement uncertainties include ± 1 mm for water elevation, ± 0.14 m/s for velocity, and less than 1% for pressure fluctuations [20]. Figures 1 and 2 illustrate the emergency gate performance of the Ghezghaleh Si and Seymareh dams at 50% openings.



Figure 1. Emergency gate performance of Ghezghaleh Si Dam at 50% openness



Figure 2. Emergency gate performance of Seymareh Dam at 50% openness

The pressure distribution and force on the High-pressure gate are influenced by various hydraulic and geometric parameters. This research aims to estimate the pressure (head) on the gate using several dimensionless predictor variables for the ANFIS model, including tunnel height upstream of the gate, gate thickness, piezometer position relative to the gate edge, gate

opening height, flow rate beneath the gate, head before the gate, tunnel width upstream, and gate edge angle.

3. Materials and methods

The artificial neural network model was introduced by McCulloch and Pitts in 1943 [21]. It can simulate any nonlinear system without prior assumptions and is effective even with incomplete or ambiguous information [22]. These networks learn from data and stored information and play a significant role in modeling, estimating, and predicting processes due to their parallel processing capabilities, intelligence, and flexibility.

The fuzzy set theory was introduced by Lotfi Zadeh at Berkeley University of America [23]. This theory can make a mathematical formulation of many concepts variables and systems that are complex and ambiguous, and provide the basis for reasoning, inference, control, and decision-making in uncertain circumstances.

Fuzzy neural systems are a combination of neural networks and fuzzy logic that has been of interest to researchers recently. Neuro-fuzzy modeling refers to the implementation of different learning techniques of artificial neural networks in fuzzy modeling or fuzzy inference systems [24]. These systems have solved the main problem in fuzzy system design (obtaining if-then rules in fuzzy systems) by making effective use of ANN learning capability to automatically generate these rules and optimize parameters.

The ANFIS model first proposed by Jang is one of the most common fuzzy-neural systems that runs a Sugeno fuzzy system in a neural structure [25]. In this model, the training process uses a combination of error propagation training methods and the least-squares error. Over the years, the ANFIS model has experienced a variety of successful applications in the aquatic sciences, including the study of runoff estimation by Kashani, and Soltangeys [26] and the Damage detection of irregular plates and regular dams by Hamidian et al. [27].

In this study, the Gaussian function was chosen from various existing fuzzy functions (triangular, trapezoidal, Gaussian, bell-shaped, etc.), with two membership functions specified for all input parameters. The general form of the used Gaussian function is as follows.

$$g(x; \sigma, c) = e^{-\frac{(x-c)^2}{2\sigma^2}} \quad (4)$$

As noted, due to the lack of direct relationships to predict and calculate the pressure distribution around the High-pressure gate, due to the influence of various parameters such as gate geometry, duct geometry before and after the gate, and hydraulic flow conditions, at first, the effective parameters became dimensionless using the dimensional analysis method and then these parameters were used to train the ANFIS system. Considering the factors affecting the pressure distribution, the following dimensional relation is suggested.

$$f(\rho, \mu, g, h_p, y_0, d, y_p, y_w, Q, H, B, \theta) = 0 \quad (5)$$

Where ρ is the fluid density, g gravity acceleration, h_p head pressure on the gate, y_0 height of the tunnel in upstream of the gate, d gate thickness, y_p position of the piezometer relative to the gate edge, y_w height of gate opening, Q discharge under the gate, h head before the gate, B tunnel width upstream of the gate, and θ angle of gate edge. The above geometrical properties are

shown in Figure 3. Using the principles of Buckingham's theory, the dimensional relation is summarized as follows:

$$f \left(\text{Re}, \frac{h_p}{H}, \sqrt[4]{\frac{Q^2}{gH^5}}, \frac{y_w}{H}, \frac{y_0}{H}, \frac{y_p}{H}, \frac{d}{H}, \frac{B}{H}, \theta \right) = 0 \quad (6)$$

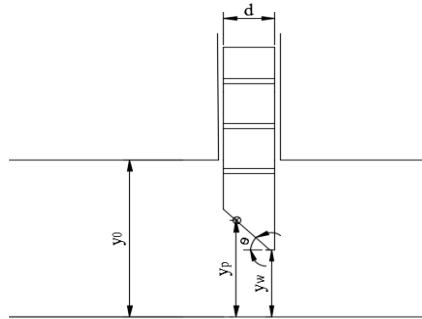


Figure 3. Geometrical parameters affecting the pressure distribution around the high-pressure gate

By combining dimensionless groups, new dimensionless parameters can be obtained as follows.

$$f^* \left(\text{Re}, \frac{h_p}{H}, \sqrt[4]{\frac{Q^2}{gH^5}}, \frac{y_w}{y_0}, \frac{y_p}{H}, \frac{d}{B}, \theta \right) = 0 \quad (7)$$

If the Reynolds number is greater than 10^5 , its effects on the model are negligible and can be ignored in the last relationship. Since the Reynolds number is greater than 10^5 , in all cases, the final relation can be expressed as follows:

$$\frac{h_p}{H} = T \left(\sqrt[4]{\frac{Q^2}{gH^5}}, \frac{y_w}{y_0}, \frac{y_p}{H}, \frac{d}{B}, \theta \right) \quad (8)$$

The scattering amplitudes of the primary variables (excluding density and viscosity) and the dimensionless parameters are summarized in Tables 1 and 2, based on the data from this study. The main parameters exhibit limited variation through dimensional analysis, allowing for accurate modeling in the ANFIS framework. Consequently, using the calculated dimensionless parameters, the training of the adaptive neural-fuzzy inference system was conducted to estimate the pressure distribution around the high-pressure gate. This pressure distribution also enables the calculation of the down-pull force applied to the gate.

Table 1. Variation domain of dimensional parameters

Parameters (Dimension)	$Q \left(\frac{m^3}{s} \right)$	H (m)	y_0 (m)	y_w (m)	y_p (m)	B (m)	d (m)	θ (degree)	h_p (m)
Minimum	7.2	30.4	1.7	0.17	0.1	1.5	0.3	45	9.2
Maximum	587.1	161.3	5.5	4.95	6.02	3.8	0.68	45	141.5

Table 2. Variation domain of dimensionless parameters

Parameters (Dimension)	$\frac{y_w}{y_0}$	$\frac{y_p}{H}$	$\sqrt[4]{\frac{Q^2}{gH^5}}$	$\frac{d}{B}$	θ	$\frac{h_p}{H}$
Minimum	0.1	0.0011	0.0078	0.13	0.785	0.28
Maximum	0.9	0.175	0.15	0.23	0.785	1.18

Model performance is evaluated using the coefficients of variation (R^2), squared mean error (RMSE), and mean relative error percentage (Error%). R^2 reflects the distribution of statistical data, while RMSE measures the discrepancy between predicted and actual values.

$$R^2 = 1 - \frac{\sum_{i=1}^n (y_{i(\text{measured})} - y_{i(\text{predicted})})^2}{\sum_{i=1}^n (y_{i(\text{measured})} - y_{i(\text{mean})})^2} \quad (9)$$

$$RMSE = \sqrt{\frac{\sum_{i=1}^n (y_{i(\text{measured})} - y_{i(\text{predicted})})^2}{n}} \quad (10)$$

$$Error\% = \frac{\sum_{i=1}^n \left| \frac{y_{i(\text{measured})} - y_{i(\text{predicted})}}{y_{i(\text{measured})}} \right|}{n} \times 100 \quad (11)$$

Where $y_{i(\text{measured})}$ is the measured pressure value in the laboratory, $y_{i(\text{predicted})}$ is the model estimate, $y_{i(\text{mean})}$ the mean pressure measured in the laboratory, and n is the number of data.

4. Results and discussion

In neural and fuzzy-neural networks, determining the network structure and selecting parameters require accurate identification of input and output parameters. For the ANFIS model to predict pressure distribution around gates effectively, data must be categorized based on the similarity of pressure distribution patterns and the underlying physics. This is contentious for two reasons: first, there is a sharp drop in pressure at the gates due to flow separation, leading to a distinct distribution compared to other gate areas. Second, the pressure distribution at 80% and 90% openings differs from that of other openings due to potential interactions between water flow and the tunnel roof, altering the flow control pattern post-gate. This behavior is evident in lab experiments and depicted in the pressure distribution diagrams around the high-pressure gate, as shown in figure 4 for the Alborz Dam service gate. The pressure distribution around the gate shows lower values at the bottom lip face. This pressure gradually increases until the end of the gate arch and then decreases with a slight slope.

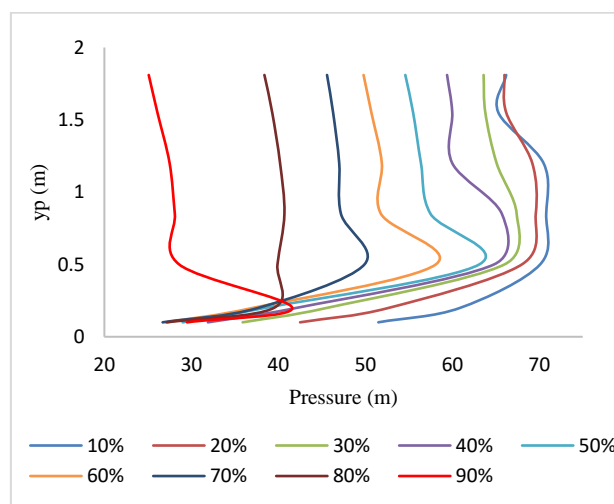


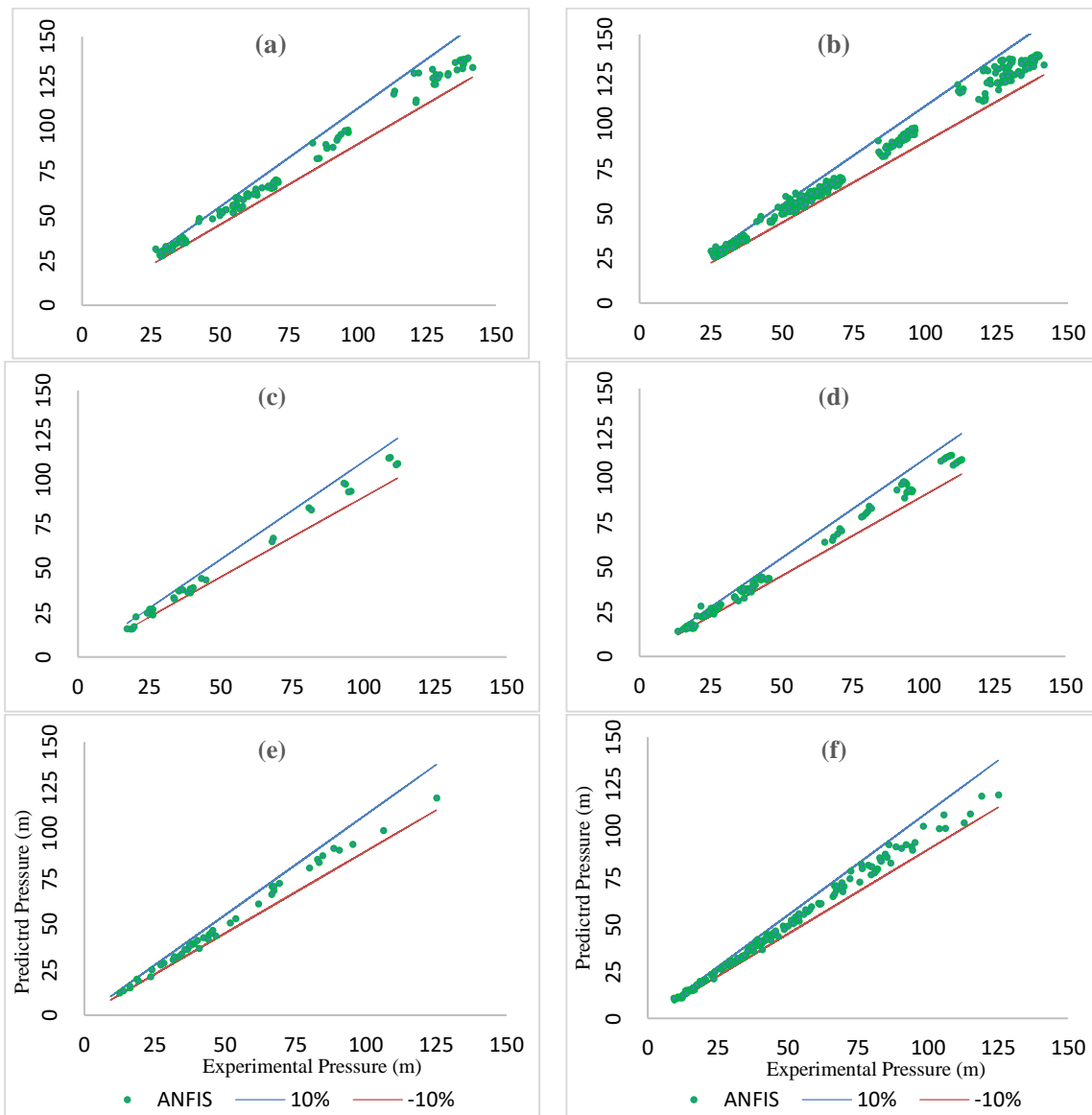
Figure 4. Pressure distribution pattern around Alborz dam service gate in different openings

To predict the pressure distribution around the high-pressure gate, three ANFIS models were employed based on the following criteria:

- Vertical and upper edge for openings of 10% to 70%
- Vertical and upper edge for openings of 80% and 90%
- Bottom edge for openings of 10% to 90%

The parameters extracted from the dimensional analysis were used as the effective variables on the pressure applied to the gate to train the ANFIS model, by explaining that 4 parameters $\sqrt[4]{Q^2 / (gH^5)}$, y_w / y_0 , y_p / H , d / B were used as input variables and h_p / H parameters as output function. It should be noted that the parameter θ had to be examined for the vertical and top edge of the gate along with the four variables mentioned for the bottom edge of the gate, but because in all models the edge angle was equal to 45, it has been neglected.

A total of 648 data points were collected to develop the Adaptive Neuro-Fuzzy Inference System (ANFIS). Each model contributed 378, 108, and 162 data points, respectively. We used 70% of each dataset for training and 30% for testing. The model results for the test and overall data for each set are shown separately in Figure 5. The relative error rate is estimated at $\pm 10\%$, as indicated in the figures. The diagrams reveal that the ANFIS model's estimated values for pressure applied to the gate mostly fall within the acceptable 10% error range, with the highest error rates observed at low pressures, particularly at 80% and 90% openings. A detailed analysis of the results reveals that most observational errors occur with low-pressure values, indicating that the estimated pressure error increases as the cavitation boundary nears. This could stem from laboratory measurement limitations. Furthermore, at 80% and 90% openings, the gate exits the bottom outlet control path, leading to greater flow turbulence and increased errors in the bottom outlet performance. The largest errors occur at the bottom lip face of the gate across all openings from 10% to 90%. These errors primarily arise from insufficient parameters for comprehensive flow modeling, such as flow separation, turbulence levels, and potential swirling flows under the gate edge, which are difficult to model accurately.



(a,c,e): ANFIS test data for vertical and top lip faces at openings of 10% to 70% vertical and top lip faces at openings of 80% and 90% Bottom lip face at openings of 10% and 90%

(b,d,f): ANFIS train and test data for vertical and top lip faces at openings of 10% to 70% vertical and top lip faces at openings of 80% and 90% Bottom lip face at openings of 10% and 90%

Figure 5. Comparison of laboratory pressure on the high-pressure gate with pressure estimated by ANFIS models

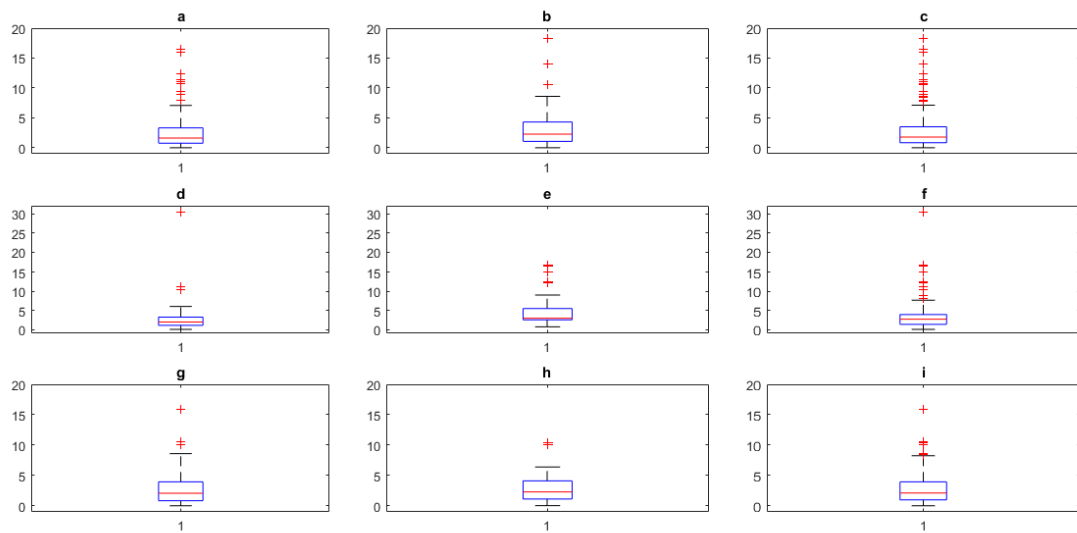
To evaluate the results more accurately, the performance of each model is assessed using the statistical parameters R^2 , RMSE, absolute relative error percentage, and maximum error, all converted to pressure dimension, as shown in Table 3. The ANFIS model demonstrates the highest accuracy for pressure measurements at the vertical and upper edges of the gate for openings between 10% and 70%. Its accuracy for pressure calculations ranges from 10% to 90% at the bottom edge and from 80% to 90% at the vertical and top edges, respectively. The mean

absolute relative errors for these models are 2.6%, 2.8%, and 3.5%. All models exhibit an R^2 coefficient close to 1, indicating strong predictability. While there are minor differences between training and test data, the overall stability indicates a robust model that generalizes effectively to new data. Although errors are typically low, the maximum error reaches 30.5% for the vertical and top lip faces at 80% and 90% openings, indicating that certain conditions may lead to less accurate predictions, necessitating further analysis of these circumstances. The table demonstrates strong model performance across various configurations, with high R^2 values and low RMSE indicating that the ANFIS models effectively estimate pressures in different settings.

Table 3. Results of ANFIS model performance in pressure estimation

Model	Method	Efficiency			
		R^2	RMSE	Error(%)	Maximom Error(%)
vertical and top lip faces at openings of 10% to 70%	Train	0.994	2.64	2.4	16.4
	Test	0.994	2.89	2.9	18.3
	All	0.994	2.71	2.6	18.3
vertical and top lip faces at openings of 80% and 90%	Train	0.996	2.02	2.8	30.5
	Test	0.995	2.26	4.8	16.6
	All	0.996	2.10	3.5	30.5
Bottom lip face at openings of 10% and 90%	Train	0.994	2.01	2.9	15.8
	Test	0.994	1.94	2.8	10.4
	All	0.994	1.99	2.8	15.8

To assess the error scattering of the ANFIS models, box diagrams for training, testing, and overall data have been created, as shown in Figure 6. Results indicate that over 75% of the data show errors below 5%, with only a small percentage exceeding 10%, reflecting the ANFIS models' desirable accuracy. The results from the box diagrams highlight both the effectiveness and limitations of the ANFIS models in estimating pressure across various configurations.



(a,d,g): ANFIS train data for vertical and top lip faces at openings of 10% to 70% vertical and top lip faces at openings of 80% and 90% Bottom lip face at openings of 10% and 90%

(b,e,h): ANFIS test data for vertical and top lip faces at openings of 10% to 70% vertical and top lip faces at openings of 80% and 90% Bottom lip face at openings of 10% and 90%

(c,f,i): ANFIS train and test data for vertical and top lip faces at openings of 10% to 70% vertical and top lip faces at openings of 80% and 90% Bottom lip face at openings of 10% and 90%

Figure 6. Absolute value box diagram of relative error of ANFIS models to estimate the pressure on High-pressure gate

The estimated pressure values are used to calculate the horizontal and vertical forces acting on the gate, which are then compared to the physical model results. The vertical force is also computed using the Nadascher relation, allowing for a comparison of the accuracy of the ANFIS method and the Nadascher relation in estimating the force on the gate. The average absolute value of the relative error is calculated, with results presented in Table 4.

Table 4. Performance results of the ANFIS model in estimating forces

Error(%)		
Fh (ANFIS)	Fv (ANFIS)	Fv (nadascher)
5.3	10.1	61.2

The estimation of forces acting on the gate based on pressures from the ANFIS model, as shown in Table 4, indicates that the horizontal force estimates are more accurate.

The greater error in estimating pressure on the bottom lip face of the gate and its pressure effect surface leads to this issue. In calculating horizontal force, the effective pressure surfaces are the vertical face and the bottom lip face; the vertical face has a larger area and a much smaller pressure error, which results in an underestimated total error for horizontal force. Conversely, because the effective pressure areas on the bottom lip face and the top of the gate are relatively equal, and the bottom lip face has a substantial error, the vertical force estimated by the ANFIS model carries a greater error than the horizontal force. The ANFIS model also

performs acceptably for vertical forces, reducing the relative error of the Nadauscher method from 61.2% to 10.1%.

Figure 7 presents the box diagram of the average absolute value of the relative error for both horizontal and vertical forces derived from the ANFIS estimated pressures. Notably, over 75% of the calculated data for both force types exhibit an error of less than 20%. The maximum estimated error for horizontal forces is around 20%, while vertical forces display greater errors, particularly at 90% openness. Since the maximum down-pull force occurs at lower openings, these larger errors can be considered negligible.

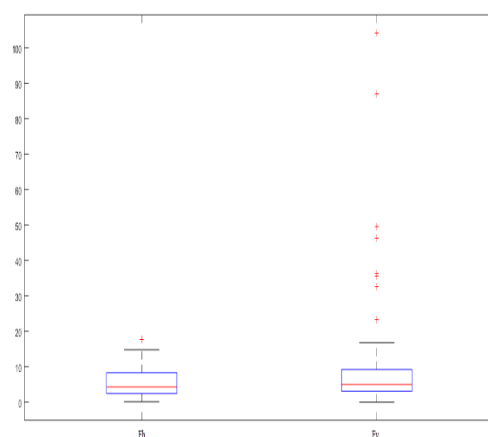


Figure 7. box Graphs of the absolute value of the relative error of horizontal and vertical forces resulting from pressure estimated by the ANFIS model

To refine the model results, apply a reliability coefficient of 1.05 for the ANFIS model's pressure distribution estimates around the Down-pull Force and horizontal force, and a coefficient of 1.2 for the vertical force on the gates, thereby enhancing the validity of the model outcomes.

To enhance the interpretability of the ANFIS model, the relationship between input parameters and output forces was explored. This allowed for a clearer understanding of how specific input variations affect the resultant forces and pressures acting on the gate. The interpretability of such predictive models is invaluable, particularly in engineering applications where decision-making relies heavily on comprehensible data analysis. The ANFIS model incorporate real-time alterations to input parameters, ensuring that the predictions remain accurate under varying conditions. In conclusion, the ANFIS model demonstrates substantial potential for predicting pressure distributions and forces on high-pressure gates. The results presented highlight its accuracy and reliability, making it a valuable tool for engineers and practitioners in hydraulic and civil engineering fields.

5. Conclusion

This paper presents a model for estimating pressure distribution around the Downpull Force of dams using an Adaptive Neuro-Fuzzy Inference System (ANFIS). The model was trained with laboratory data from physical models of the Ghezghaleh Si, Alborz, Gotvand, Namroud, and Seymareh dams, totaling 648 data points obtained from the Iran Water Research Institute. Analysis revealed that pressure distribution in the vertical direction for 80% and 90% openings

differs from other openings. Additionally, flow separation at the gate edge causes a sharp pressure drop, prompting the use of three models for accurate pressure estimates. The ANFIS model's predictions for high-pressure gates were compared with actual data, demonstrating its superiority over conventional methods. Utilizing the estimated pressure values from ANFIS, the horizontal and vertical forces on the high-pressure gates across different openings were calculated and compared with laboratory results and the Naudascher relationship (vertical force only). The findings indicate that the ANFIS model effectively estimates both horizontal and vertical forces on the gates. A key advantage of this model is its ability to estimate horizontal forces, which have traditionally required laboratory testing. The model's high accuracy supports its preference for designing high-pressure gate elevator jacks over standard methods and previous laboratory or numerical studies.

References

1. Jamali Rovesht, T., & Manafpour, M. (2019). "Investigation on cavitation occurrence potential in Seymareh dam's bottom outlet." *ISH Journal of Hydraulic Engineering*, 1-12.
2. Salazar, F., San-Mauro, J., Celigueta, M. Á., & Oñate, E. (2017). "Air demand estimation in bottom outlets with the particle finite element method." *Computational Particle Mechanics*, 4(3), 345-356.
3. Ruan, S. P., Wu, J. H., Wu, W. W., & Xi, R. Z. (2007). "Hydraulic research of aerators on tunnel spillways." *Journal of Hydrodynamics*, 19(3), 330-334.
4. Ghazali, F., Salehi Neyshabouri, S. A. A., & Kavianpour, M. R. (2015). "The effect of bottom outlet geometry changes on hydraulic characteristics of flow." *Modares Civil Engineering journal*, 15(3), 171-182.
5. Aydin, I., Telci, I. T., & Dundar, O. (2006). "Prediction of downpull on closing high head gates." *Journal of Hydraulic Research*, 44(6), 822-831.
6. Ahmed, T. M. (2017). "Effects of Gate Lip Shapes on Hydrodynamic Forces on Gate Dam Tunnels." *Eurasian Journal of Science & Engineering*, 3(2), 47-57.
7. Naudascher, E., Kobus, H., & Rao, R. P. R. (1964). "Hydrodynamic analysis for high-head leaf gates."
8. Sagar, B. (1977). "Downpull in High-head Gate Installations, Parts 1, 2, 3." *Water Power Dam Construct*, (3), 38-39; (4), 52-55; (5), 29-35.
9. Sagar, B.T.A. and Tullis, J.P. (1979). "Downpull on Vertical Lift Gates". *Water Power Dam Construct*. 12, 35-41.
10. Naudascher, E. (1991). "Hydrodynamic forces." CRC Press LLC.
11. Amorim, J. C. C., & de Andrade, J. L. (1999). "Numerical analysis of the hydraulic downpull on vertical lift gates." In *Waterpower'99: Hydro's Future: Technology, Markets, and Policy* (pp. 1-9).
12. Sagar, B. T. A. (1999, August). "Gate lip hydraulics." In *1999 IAHR Congress Proceedings Graz*. Austria: IAHR.
13. Alhashimi, S. A., Al-Kifae, M. T., & Almaini, R. M. (2010). "Prediction downpull force on tunnel gate with different gate lip geometry." *journal of kerbala university*, 8(4), 273-288.
14. Markovic-Brankovic, J., & Drobier, H. (2013). "New high head leaf gate form with smooth upstream face." *Tem Journal*, 3.

15. Taher, T. M., & Anwar, A. O. (2016). "Effects of gate lip orientation on bottom pressure coefficient of dam tunnel gate." *Arabian Journal for Science and Engineering*, 41(12), 4927-4936.
16. Ameen, S., Taher, T., & Ahmed, T. M. (2018). "Effects of Geometrical and Flow Rates on the Prediction of Bottom Pressure Coefficients of Tunnel Lift Gate of Dams." *Journal of The Institution of Engineers (India): Series A*, 99(4), 741-749.
17. Mohammed, B. T., & Ali, B. M. A. S. (2018a). "Numerical Investigations of Downpull Forces for leaf gate in high dams." *ZANCO Journal of Pure and Applied Sciences*, 30(1), 76-82.
18. Mohammed, B. T., & Ali, B. M. A. S. (2018b). "Simulation of Downpull Forces of Leaf Gate in High Dams." *ZANCO Journal of Pure and Applied Sciences*, 30(1), 16-23.
19. Sajadi, H.R. Kavianpour, M.R. (2019). "Evaluation of pressure distribution around high pressure gates of dams using artificial neural network method." 15th National Congress of Civil Engineerin, Shiraz, Iran. (In Persian).
20. Aminoroayaie Yamini, O., Kavianpour, M. R., Mousavi, S. H., Movahedi, A., & Bavandpour, M. (2018). Experimental investigation of pressure fluctuation on the bed of compound flip buckets. *ISH Journal of Hydraulic Engineering*, 24(1), 45-52.
21. McCulloch, W. S., & Pitts, W. (1943). "A logical calculus of the ideas immanent in nervous activity." *The bulletin of mathematical biophysics*, 5(4), 115-133.
22. ASCE Task Committee on Application of Artificial Neural Networks in Hydrology. (2000). Artificial neural networks in hydrology. II: Hydrologic applications. *Journal of Hydrologic Engineering*, 5(2), 124-137.
23. Lotfi Zadeh, A. (1965). "Fuzzy sets." *Information and control*, 8(3), 338-353.
24. Aqil, M., Kita, I., Yano, A., & Nishiyama, S. (2007). "Analysis and prediction of flow from local source in a river basin using a Neuro-fuzzy modeling tool." *Journal of environmental management*, 85(1), 215-223.
25. Jang, J. S. (1993). "ANFIS: adaptive-network-based fuzzy inference system." *IEEE transactions on systems, man, and cybernetics*, 23(3), 665-685.
26. Kashani, M. H., & Soltangeys, R. (2018). Comparison of three intelligent techniques for runoff simulation. *Civil Engineering Journal*, 4(5), 1095-1103.
27. Hamidian, D., Salajegheh, J., & Salajegheh, E. (2018). Damage detection of irregular plates and regular dams by wavelet transform combined adoptive neuro fuzzy inference system. *Civil Engineering Journal*, 4(2), 305-319.



© 2025 by the authors. Licensee SCU, Ahvaz, Iran. This article is an open access article distributed under the terms and conditions of the Creative Commons Attribution 4.0 International (CC BY 4.0 license) (<http://creativecommons.org/licenses/by/4.0/>).

